

Low-lying excitations and magnetization process of coupled tetrahedral systems

K. Totsuka^{1,*} and H-J. Mikeska¹

¹*Institut für Theoretische Physik, Universität Hannover, Appelstr. 2, 30167 Hannover, Germany*

(Dated: September 2001)

We investigate low-lying singlet and triplet excitations and the magnetization process of quasi-1D spin systems composed of tetrahedral spin clusters. For a class of such models, we found various exact low-lying excitations; some of them are responsible for the first-order transition between two different ground states formed by local singlets. Moreover, we find that there are two different kinds of magnetization plateaus which are separated by a first-order transition.

PACS numbers: 75.10.Jm, 75.60.Ej, 75.40.-s

I. INTRODUCTION

Recently, there has been substantial interest in the properties of strongly frustrated low-dimensional quantum spin systems such as $S = 1/2$ Heisenberg models on the kagomé and pyrochlore lattices. In such systems, various ground-state phases, *e.g.* valence-bond crystals, RVB, long-range ordered phases etc, appear as we vary the control parameters. In particular, the possibility of a spin-liquid phase with unconventional singlet excitations would be interesting¹.

In the following, we consider a simple model system built up from tetrahedral clusters of $S = 1/2$ (we label each tetrahedron by Latin indices j) with the Hamiltonian (see Fig.1)

$$\begin{aligned} \mathcal{H}_0 = & \sum_j J_1 (\mathbf{S}_{j,1} \cdot \mathbf{S}_{j,3} + \mathbf{S}_{j,2} \cdot \mathbf{S}_{j,4}) \\ & + \sum_j J_2 (\mathbf{S}_{j,1} \cdot \mathbf{S}_{j,2} + \mathbf{S}_{j,2} \cdot \mathbf{S}_{j,3} + \mathbf{S}_{j,3} \cdot \mathbf{S}_{j,4} + \mathbf{S}_{j,4} \cdot \mathbf{S}_{j,1}) . \end{aligned} \quad (1)$$

These tetrahedra form a chain-like structure and interact with each other by the following coupling:

$$\begin{aligned} \mathcal{H}_1 = & \sum_j [J_3 (\mathbf{S}_{j,2} \cdot \mathbf{S}_{j+1,3} + \mathbf{S}_{j,4} \cdot \mathbf{S}_{j+1,1}) \\ & + J_4 (\mathbf{S}_{j,2} \cdot \mathbf{S}_{j+1,1} + \mathbf{S}_{j,4} \cdot \mathbf{S}_{j+1,3})] . \end{aligned} \quad (2)$$

For $J_2 = J_3 = J_4$, this model reduces to a known model of a frustrated spin ladder with diagonal couplings ('generalized Bose-Gayen model'^{2,3}). The choice $J_3 = J_4 \neq J_2$ (*symmetric model*, hereafter) introduces explicit dimerization in the leg direction. As can be seen in Fig. 2, an assembly of decoupled tetrahedra described by \mathcal{H}_0 has singlet modes with energies much lower than the singlet-triplet gap. Therefore, the model with $J_1, J_2 \gg J_3, J_4$ would provide a good starting point to study the unconventional properties mentioned above.

The study of the model described by the Hamiltonian $\mathcal{H}_{\text{tot}} \equiv \mathcal{H}_0 + \mathcal{H}_1$ was inspired by the discovery of the tellurate materials⁴ $\text{Cu}_2\text{Te}_2\text{O}_5\text{X}_5$ ($\text{X} = \text{Cl}$ or Br) and the phase diagram, triplet excitations, and the optical spectrum of this model have been investigated quite

recently⁵ using both numerical diagonalization and the bond-operator mean-field approximation. In these materials, Cu^{2+} ions form $S = 1/2$ tetrahedra, which are connected with each other by Te-O coordinations. Although the coupling between the tetrahedra is not so simple, the crystal structure⁴ (P4) suggests that the model Hamiltonian \mathcal{H}_{tot} with $J_3 = J_4$ is one of the simplest candidates to describe the tellurates (the chain axis is parallel to c -axis of the tellurates). On the basis of experimental results obtained for static magnetic properties⁴ and for Raman scattering⁶, it was argued that the parameters $J_1 \approx J_2$ and $J_3 = J_4 \ll J_1$ may be appropriate for the two compounds. We will also include some results for a more general case with $J_3 \neq J_4$ (hence we call it *generalized model* in the following) which may clarify to what extent our results are general.

Our aim here is to investigate (i) general excited states and their relation to the ground-state phase transitions and (ii) the magnetization plateaus. In what follows, we will use eigenstates of the four $S = 1/2$ spins on a single tetrahedron in the notation as shown in Fig.3. The ground state of the chain of non-interacting tetrahedra $J_3 = J_4 = 0$ is obtained as a sequence of tetrahedra in state '1' for $J_1 > J_2$ and as that of tetrahedra in state '2' for $J_1 < J_2$.

We conclude this introduction with a few comments on the ground state phase diagram for the symmetric model (including the coupling $J_3 = J_4$) which was investigated already in Ref. 5. The main purpose of this part consists not in obtaining the phase diagram itself but in demonstrating how the low-lying singlets dictate the transition. To discuss the structure of the phase diagram from the viewpoint of the singlet spectra, we use an effective Hamiltonian derived by paying particular attention to low-energy singlets. This approach gives a simple and clear picture of the transition between singlet phases and will be useful also for a discussion of the low-energy singlet dynamics.

The classical model ($S \nearrow \infty$) has two different kinds of antiferromagnetic phases separated by a line $J_1 = J_2 + J_3$. Along the transition line, the ground state exhibits a huge degeneracy, which is reminiscent of what occurs to the classical pyrochlore antiferromagnets¹. As was already pointed out in Ref. 5, the symmetric model ($S = 1/2$)

preserves the basic property⁷ of the generalized Bose-Gayen model: the total spins $\mathbf{S}_{j,1} + \mathbf{S}_{j,2}$ and $\mathbf{S}_{j,3} + \mathbf{S}_{j,4}$ on individual dimer bonds (J_1) are well-defined quantum numbers. This allows a simple classification of the eigenstates of \mathcal{H}_{tot} by specifying these quantum numbers for all $2N$ (N : the number of tetrahedra) dimer bonds. When all dimers are occupied by triplets, the Hamiltonian \mathcal{H}_{tot} reduces to an effective spin-1 chain²:

$$\mathcal{H}^{S=1} = J_2 \sum_{k: \text{ odd}} \mathbf{T}_k \cdot \mathbf{T}_{k+1} + J_3 \sum_{k: \text{ even}} \mathbf{T}_k \cdot \mathbf{T}_{k+1}, \quad (3)$$

where \mathbf{T}_k denotes an effective spin-1 operator $\mathbf{S}_{1, \frac{k+1}{2}} + \mathbf{S}_{3, \frac{k+1}{2}}$ (for k : odd) or $\mathbf{S}_{2, \frac{k}{2}} + \mathbf{S}_{4, \frac{k}{2}}$ (for k : even). On the other hand, interactions J_2 and J_3 effectively vanish when all dimer bonds are occupied by singlets.

It was argued in Ref. 5 that the quantum phase diagram contains three different phases: rung-dimer (RD), Haldane⁸ (H), and spin-1 dimerized (S1D, or plaquette singlet) phase^{9,10}; the first one is characterized by the formation of local singlets on dimer (J_1) bonds. On the other hand, the latter two are phases of the model $\mathcal{H}^{S=1}$ (eq.(3)) and are distinguished¹⁰ according to whether the string-order parameter¹¹ is vanishing or not. Note that we can use a variational argument to show *rigorously* that RD phase actually realizes *at least* for $J_1 > J_2 + J_3$ ($J_2, J_3 > 0$) in the sense that no admixture of singlets ‘1’ and ‘2’ occurs.

To investigate the effect of the coupling J_3 between tetrahedra on low-lying singlets analytically, we derive an effective Hamiltonian acting on the 2^N -dimensional subspace spanned by two nearly degenerate states ‘1’ and ‘2’. At ‘site’- j (i.e. j -th tetrahedron), we define an Ising spin with a value $+1$ (-1) when the tetrahedron is in state ‘2’ (‘1’). The coupling between tetrahedra is taken into account by degenerate perturbation theory and the resulting effective Hamiltonian is given by a ferromagnetic Ising chain in an external field:

$$\mathcal{H}_{\text{Ising}} = J_{\text{IM}} \sum_j \sigma_j \sigma_{j+1} - h_{\text{IM}} \sum_j \sigma_j. \quad (4)$$

with

$$J_{\text{IM}} = -\frac{J_3^2}{6J_2}, \quad h_{\text{IM}} = J_2 - J_1 + \frac{J_3^2}{3J_2}. \quad (5)$$

We have different ground states according to the sign of the effective magnetic field h_{IM} : For $h_{\text{IM}} < 0$ the Ising spins align downward and the ‘rung dimer (RD)’ phase realizes, while a positive value of h_{IM} makes Ising spins point upward to form the ‘spin-1 dimer (S1D)’ phase. The condition $h_{\text{IM}} = 0$ determines the line of first-order transition between the RD- and the S1D phase. The mechanism of the transition will be discussed in the next section from the viewpoint of the excitation spectra. In Fig.4, we show the transition line obtained above by a solid line. This result implies that at the symmetric point $J_2/J_1 = 1$ a small perturbation J_3 resolves the

huge degeneracy and S1D phase is selected as a unique, spin-singlet ground state.

The explicit form of the ground state is known analytically in the whole RD phase (all tetrahedra in state ‘1’) and only on the line $J_3 = 0, J_2 > J_1$ in the S1D phase (all tetrahedra in state ‘2’). In the remaining part of the phase diagram, the ground state is known numerically from the study of $S = 1$ -chains with alternating exchange^{9,10}. In particular the separation line between the Haldane and the S1D phase is given by $J_3/J_2 \approx 0.6$, where a second-order transition described by the $\theta = \pi$ O(3) non-linear sigma model⁸ occurs. The quantum critical point, where all three phases meet and the gap of the first order transition disappears, is of particular interest, but will have to be treated beyond perturbation theory. In section IV, we briefly discuss the effect of *interchain* couplings in conjunction with three-dimensional ordering.

As an independent check of our method, we also determined the RD-S1D boundary by adapting numerical data of Ref. 10 (open squares in Fig. 4. Note that this is essentially the same as that given in Ref. 5). The resulting ground-state phase diagram is shown in Fig. 4 as a function of J_2/J_1 and J_3/J_1 with J_1 as the energy unit. The merit of this representation is that the phase diagram clearly exhibits the symmetry under the exchange of J_2 and J_3 . In the inset, we also show the same data in the $(J_3/J_2, J_1/J_2)$ -plane, the parametrization used in a recent literature⁵, in order to facilitate a comparison. Although we used a completely different method, the result is consistent with the one obtained by the bond-operator mean-field approach⁵. The inclusion of higher-order terms hardly changes the boundary and we may expect that the convergence of our calculation is good. We would like to stress here that our simple effective Hamiltonian (4) not only yields a fairly good result¹² but also gives us a clear picture of the transition as will be described in the next section.

For the generalized model, the phase diagram is not symmetric and the relation to spin-1 chains is no longer useful. For small J_3 (or equivalently, J_4), however, the mapping to the Ising chain (4) goes in a similar manner to give

$$J_{\text{IM}} = -\frac{(J_1 - 3J_2)^2 J_3^2}{48J_1(2J_2 - J_1)J_2}, \quad h_{\text{IM}} = J_2 - J_1 + \frac{(2J_1 - 3J_2)(J_1 - 3J_2)}{24J_1J_2(J_1 - 2J_2)} J_3^2. \quad (6)$$

Setting $J_1 = J_2$, we obtain a negative value $h_{\text{IM}} = -J_3^2/(12J_1)$. Contrary to the previous case (symmetric model), this implies that for perfect ($J_1 = J_2$) tetrahedra the inter-tetrahedron coupling selects not the S1D ground state but the RD one. The results obtained in this section lead us to conclude that *if the value $J_1 = J_2$ is reliable for the real compounds $\text{Cu}_2\text{Te}_2\text{O}_5\text{X}_2$ ($\text{X}=\text{Cl}, \text{Br}$), they should be treated in the S1D phase.*

II. EXCITATIONS

Because of the fully frustrated tetrahedral structure, there are various types of singlet and triplet excitations. Among them, singlet excitations within the triplet gap are of particular interest^{13,14,15}. Main results of this section are summarized in Figs. 5, 6 and Table I.

A. Excitations in the rung-dimer phase

1. Singlet excitations

As can be easily seen from Fig.2, low-lying singlet degrees of freedom do exist in the neighborhood of the point $J_1 = J_2$ which corresponds to perfect tetrahedra. The lowest singlet in the rung-dimer (RD) phase is created by promoting one of the RD tetrahedra to an S1D singlet (state ‘2’ in Fig.3). For the symmetric model, this is an exact eigenstate with energy $2(J_1 - J_2)$ since the interaction Hamiltonian \mathcal{H}_1 annihilates this state. For an estimate of the interaction effects ($\propto J_3$), the effective Hamiltonian (4) can be used and leads to the results:

$$\begin{aligned} \Delta_{\text{RD}}^{\text{sing}} &= 2(J_1 - J_2) \quad \text{for the symmetric model,} \\ \Delta_{\text{RD}}^{\text{sing}} &= 2(J_1 - J_2) + \frac{J_3^2}{4} \left(\frac{3}{4J_1} - \frac{1}{4J_2} \right) \\ &\quad \text{for the generalized model.} \end{aligned} \quad (7)$$

Alternatively this state can be viewed as a singlet bound state made up of two dimer triplets in the dimer region ($J_1 \gg J_2$). The expression for the generalized model (second eq. of (7)) is, of course, not exact, but we can show, at least in a perturbative sense, that this excitation is completely localized (i.e. dispersionless) also in the generalized model.

What is more interesting is that there exist multiparticle bound states which is given by $n(\geq 2)$ successive S1D singlets; ferromagnetic interaction in the effective Hamiltonian provides the attraction between these particles (the binding energy is $-4(n-1)|J_{\text{IM}}|$). For both symmetric- and generalized models, the total energy of this kind of bound states is given by

$$\Delta_{n\text{-bound}}^{\text{RD}} = \Delta_{\text{RD}}^{\text{sing}} + 2(n-1)|h_{\text{IM}}|. \quad (8)$$

Thus, when the phase boundary is approached from the RD side ($h_{\text{IM}} \rightarrow -0$), all these bound states collapse onto the lowest singlet (while a small gap of order $J_1 - J_2$ remains between the singlet ground state and the lowest singlet excitation—see Fig.5). This collapse triggers phase separation and leads to the first-order transition from singlet RD to singlet S1D. In particular, the largest one with the gap $\Delta_{\text{RD}}^{N\text{-bound}} = 2N|h_{\text{IM}}|$ hits the ground state at the transition point and after the transition these huge bound states constitute low-lying excitations of the new phase. Contribution of these low-lying singlets to such

physical quantities as specific heat can be calculated by using the solvable Hamiltonian $\mathcal{H}_{\text{Ising}}$.

On top of them, there are several singlet bound states composed of two *triplet* tetrahedra. For example, a singlet combination of two triplet tetrahedra (state ‘ α ’ and ‘ β ’) connected by a weak (J_3) link has an exact energy $2J_1 - 2J_3$, which lies between the two-triplet threshold $2J_1$ and the elementary singlet $\Delta_{\text{sing}}^{\text{RD}}$.

2. Triplet excitations

In this subsection, we discuss several exact magnetic excitations for the symmetric model. Although most of the following results hold also for the generalized model, the excited states are no longer exact.

The simplest such excitation is an immobile dimer triplet excitation created by replacing one of the singlet (state ‘1’) tetrahedra by a tetrahedron in state ‘ α ’ or ‘ β ’. The exact excitation energy is J_1 , independent of J_2 and J_3 . These are nothing but dimer-triplet excitations of the standard two-leg ladder with Bose-Gayen type couplings.

Another triplet with energy $2J_1 - J_2$ can be created by promoting one tetrahedron from state ‘1’ to state ‘ γ ’, composed of two dimer triplets. In the dimer limit ($J_1 \gg J_2, J_3$), this state can be viewed as a triplet bound state made up of two dimer triplets (with binding energy $-J_2$). If two dimer triplets are bound on a weak (J_3) link, then they form another exact bound state with energy $2J_1 - J_3$, corresponding to adjacent tetrahedra in states ‘ α ’ and ‘ β ’. By a logic similar to that used in the previous subsection (section II.A.1), we can show that these triplets are completely localized (i.e. dispersionless) even if we relax the condition $J_3 = J_4$.

B. Excitations in the $S = 1$ dimer phase

1. Singlet excitations

Starting from the ground state of the S1D phase, elementary singlet excitations for the symmetric model are obtained by changing some tetrahedra to state ‘1’. Since the intertetrahedra coupling \mathcal{H}_1 annihilates links with at least one tetrahedron in state ‘1’ on their edges, this change results in a sequence of finite $S = 1$ chains. The excitation energy, however, cannot be calculated analytically because of quantum fluctuation coming from $S = 1$ segments. For the lowest singlet excitation, obtained for one tetrahedron in state ‘1’, the energy is obtained in second-order perturbation as (the second-order correction in the following expression is the contribution from the open ends of two $S = 1$ chains)

$$\Delta_{\text{S1D}}^{\text{sing}} = 2(J_2 - J_1) + 4J_3^2/(3J_2);$$

We have $\Delta_{\text{S1D}}^{\text{sing}} > 0$ in the S1D phase. It is easy to verify that $\Delta_{\text{S1D}}^{\text{sing}}$ coincides with the first equation of (7) at the

transition point $|h_{\text{IM}}| = 0$.

As in the case of the RD phase, we can consider several multiparticle states made up of state ‘1’ tetrahedra (both scattering states and bound states). Among them, the most important is an n -particle bound state. The energy of immobile n -particle bound states can be calculated in perturbation theory as

$$\Delta_{\text{S1D}}^{\text{sing}} + 2(n-1)h_{\text{IM}}.$$

Again, when $h_{\text{IM}} \approx 0$, the binding energy is so large that all multiparticle bound states have the same energy $\Delta_{\text{S1D}}^{\text{sing}}$. This is the origin of instability towards the first-order transition from the S1D to the RD. It is important to note that all the above excitations are *not* included in the effective spin-1 chain, but correspond to an internal degree of freedom on a pair of dimer spins.

2. Triplet excitations

Two different types of triplet excitations exist. The first one is essentially a single tetrahedron in state-‘ α ’(‘ β ’) in the S1D background; it creates a single dimer singlet in the sea of dimer triplets and is *not* included in the usual ‘ $S = 1$ chain’. This is highly localized because an ‘unpaired’ spin-1 object appearing at the edge of the effective $S = 1$ chain (with an odd number of effective spins) can hardly move due to strong dimerization¹⁹. The energy is given by

$$\Delta_{\text{type-1}}^{\text{triplet}} = -J_1 + 2J_2 + O(J_3^3).$$

Triplet excitations of the second type are contained in the excited states of ‘ $S = 1$ chain’ and are obtained by promoting a single tetrahedron to state-‘ γ ’. The excitation discussed in Ref. 5 by a mean-field approximation etc. is of this type. Contrary to the ‘ γ ’ tetrahedron in the RD phase, this magnon excitation can propagate freely due to the ‘background’ of dimer triplets and the dispersion is given by

$$\begin{aligned} \omega_{\text{type-2}}^{\text{triplet}}(q) &= \left(J_2 + \frac{8J_3^2}{27J_2} \right) - \left(\frac{4J_3}{3} + \frac{2J_3^2}{3J_2} \right) \cos q - \frac{4J_3^2}{9J_2} \cos 2q. \end{aligned} \quad (9)$$

Note that this has a relatively large bandwidth of $0.92J_1$ (for $J_1 = J_2$ and $J_3/J_1 = 0.3$). This fact shows that the effect of intertetrahedra couplings on low-lying excitations is drastically different according to the spin background. This difference may be crucial also in considering possible scenario of three-dimensional ordering (see sectionIV).

Furthermore, by solving a two-magnon problem explicitly²⁰, we found singlet- and triplet bound states around $q = \pi$, whose binding energies are a few percent

of the triplet gap. The singlet one agrees qualitatively with that pointed out in Ref.5 in conjunction with the Raman spectrum. The detail will be reported elsewhere.

Because of the large bandwidth, a crossing between the type-2 mobile triplet and the lowest gapped singlet (state-‘1’) occurs at relatively small value of J_2/J_1 (1.47 for $J_3/J_1 = 0.3$). For $0.5 < J_2/J_1 < (J_2/J_1)_{c2}$, the system is *unusual* in the sense that the ground state is dimer-like or $S = 1$ -like while the singlet-triplet gap is filled with many low-lying singlets. For larger values of J_2 , the tetrahedral chain is equivalent to a standard $S = 1$ chain not only for the ground state but also for low-lying excitations.

We summarize the results obtained in this section in Fig.5, 6 and Table I. In Fig.5, we can see clearly the collapse of a huge number of singlet states mentioned above. Among them, the longest one (which is not shown here) comes down from infinitely high energies and hits the RD ground state at $J_2/J_1 = (J_2/J_1)_{c1}$. In Fig.6, some triplet branches appear discontinuous at the transition. This is because the corresponding state acquires an extensive dispersion when the critical value $J_2 = J_{2c}$ is crossed from the RD side. The difference between a given type of excitation in a ‘background’ of states ‘1’ and ‘2’ respectively, i.e. the discontinuity appearing in Fig.6, vanishes as the coupling J_3 decreases. For example, the level corresponding to the gap $\Delta_{\text{triplet}}^{\text{type-1}}$ has a discontinuity²¹ of the order J_3^2 .

III. MAGNETIZATION PROCESS

In this section, we investigate the magnetization process of the tetrahedral chain for fields up to the saturation field, paying particular attention to the magnetization plateaus which appear at $m^z/m_{\text{sat}} = 1/2$ and are related to two different quantum states. Since the real materials have $J_1 \approx J_2 \approx 40$ K, these plateaus may be detected in high-field magnetization measurements.

The appearance of two different types of plateaus at $m^z/m_{\text{sat}} = 1/2$ is apparent already in the limit of isolated tetrahedra (i.e. $J_3 = 0$); for $J_2 < J_1$ this plateau occurs for magnetic fields $J_1 < H < J_1 + J_2$ and with the system either in state ‘3’ or in state ‘6’ (type I plateau), whereas for $J_2 > J_1$ the plateau occurs for magnetic fields $J_2 < H < 2J_2$ with the system in state ‘9’ (type II plateau).

For a discussion of the magnetization process in the presence of interaction ($J_3 \neq 0$), we start by considering the dimer limit $J_1 \gg J_{2,3}$ where the plateau of type I is realized. It is well-known that the magnetization process in this limit can be reduced to that of an effective $s = 1/2$ model²⁵ by regarding a triplet on a dimer bond as an upward spin ($s^z = +\frac{1}{2}$) and, correspondingly, a singlet as downward spin ($s^z = -\frac{1}{2}$). The effective Hamiltonian obtained in this way is

$$\begin{aligned} \mathcal{H}_{\text{eff-1}} = & \sum_{(i,i+1) \in \text{between tetra.}} [J_{xy}(s_i^x s_{i+1}^x + s_i^y s_{i+1}^y) + J_{zz} s_i^z s_{i+1}^z] + J_2 \sum_{(j,j+1) \in \text{tetra}} s_j^z s_{j+1}^z \\ & - (H - J_1 - \frac{1}{2}J_{zz} - \frac{1}{2}J_2) \sum_k s_k^z, \end{aligned} \quad (10)$$

where J_{xy} and J_{zz} are

$$J_{xy} = \begin{cases} 0 & \text{for symmetric model} \\ J_3 & \text{for generalized model} \end{cases}, \quad J_{zz} = \begin{cases} J_3 & \text{for symmetric model} \\ J_3/2 & \text{for generalized model} \end{cases}. \quad (11)$$

When J_2 is sufficiently larger than J_3 , crystallization of upward spins (or, hardcore bosons) occurs and a ‘solid’ phase ...333333... or ...666666... is realized. Note that both states spontaneously break link-parity (translational symmetry is not broken). While this crystallization is obvious for the symmetric model, the situation is slightly subtle for the generalized model since the coupling between tetrahedra is XY-like. Fortunately, even in this case we can show that either of the two is selected by a weak J_3 -coupling.

In order to excite this ‘crystallized’ ground state *magnetically*, a finite amount of energy ($\propto J_2 + J_3$) has to be spent and this leads to the type-I plateau at $m^z/m_{\text{sat}} = 1/2$. In particular, it is clear from the absence of any kind of kinetic terms that the magnetization process for the symmetric model is step-like²² under the conditions assumed here ($J_1 \gg J_2, J_3$).

As is obvious from Fig. 3, for $J_1 \approx J_2$ two different magnetic particles (‘3’ or ‘6’ and ‘9’) degenerate and competition between two different plateau phases (type-I and II) occurs. To investigate it, we can use a similar method to that used in section I for $J_2 \approx J_1$ and $J_3 \ll J_1, J_2$. Let us fix the magnetization $m^z/m_{\text{sat}} = 1/2$. Then the half magnetized state is dominated by the three types of tetrahedra triplets ‘3’, ‘6’ and ‘9’ and we can construct an effective $S = 1$ Hamiltonian using these nearly degenerate states. We identify the tetrahedron states $\frac{1}{\sqrt{2}}(|'3'\rangle \pm |'6'\rangle)$ and $|'9'\rangle$ with $S^z = \pm 1$ and $S^z = 0$, respectively, and obtain, in lowest non-trivial order, the following effective Hamiltonian:

$$\begin{aligned} \mathcal{H}_{\text{eff-2}} = & -\frac{J_3}{4} \sum_j [(\tilde{S}_j^x)^2 - (\tilde{S}_j^y)^2] [(\tilde{S}_{j+1}^x)^2 - (\tilde{S}_{j+1}^y)^2] \\ & + (J_2 - J_1) \sum_j (\tilde{S}_j^z)^2. \end{aligned} \quad (12)$$

It is clear that the above model has two phases: when J_3 is much larger than $J_2 - J_1 (> 0)$, the ground state is given by a product $\otimes_j \frac{1}{\sqrt{2}}(|'3'\rangle_j \pm |'6'\rangle_j)$ while the trivial product $\otimes_j |'9'\rangle_j$ becomes the ground state when $(\tilde{S}^z)^2$ is dominant.

If we notice that the above model is in fact classical, it is not difficult to know what kind of transition occurs be-

tween two phases. Although the Hamiltonian (12) looks complicated, the fact that $[(\tilde{S}_j^x)^2 - (\tilde{S}_j^y)^2, (\tilde{S}_j^z)^2] = 0$ enables us to rewrite it in terms of classical spins σ_j which take three values $-1, 0$, and 1 . That is, if we identify $\frac{1}{\sqrt{2}}(|'1'\rangle \pm |'-1'\rangle)$ and $|'0'\rangle$ with $\sigma = \pm 1$ and $\sigma = 0$ respectively and perform the replacement

$$\sigma_j = (\tilde{S}_j^x)^2 - (\tilde{S}_j^y)^2, \quad \sigma_j^2 = (\tilde{S}_j^z)^2, \quad (13)$$

the Hamiltonian (12) reduces to

$$\mathcal{H}'_{\text{eff-2}} = -\frac{J_3}{4} \sum_j \sigma_j \sigma_{j+1} + (J_2 - J_1) \sum_j \sigma_j^2. \quad (14)$$

This is nothing but the Blume-Capel model whose phase diagram is well known²³; for sufficiently low temperatures (zero, in our case), there are a ferromagnetic phase with all σ taking 1 or -1 and the so-called vacancy phase where $\sigma = 0$ at all sites and these two phases are separated by a first-order transition. In the language of the original quantum spins, the ferromagnetic state corresponds to $\otimes_j |'3'\rangle_j$ or $\otimes_j |'6'\rangle_j$ and the vacancy state to $\otimes_j |'9'\rangle_j$. Therefore, the aforementioned two plateau phases correspond to the ferromagnetic- and the vacancy phases, respectively.

The above argument is based on the lowest-order effective Hamiltonian. If we proceed to the next order, a new interaction appears:

$$\sum_j \sigma_j \sigma_{j+1} (\sigma_j - \sigma_{j+1}). \quad (15)$$

Fortunately, this type of interactions does not affect the two phases mentioned above and we may expect that our result will remain qualitatively correct in higher orders of perturbation theory.

We determine the phase boundary by perturbation expansion. By comparing the energies of both states obtained by perturbation expansion (up to second order), we obtain the following equation for the phase boundary

$$J_1 - J_2 + \frac{1}{4}J_3 - \frac{53J_3^2}{64J_2} = 0. \quad (16)$$

The leading term $J_1 - J_2 + J_3/4$ coincides with that given by eq.(14). In Fig.7 we show the phase diagram for finite magnetization $m^z/m_{\text{sat}} = 1/2$. Inside the boundary, we have parity breaking states (...33333... or ...66666...) similar to that found in Ref.25 and a unique parity-symmetric state (...99999...) outside.

IV. SUMMARY AND DISCUSSION

Motivated by recent discovery of tellurates $\text{Cu}_2\text{Te}_2\text{O}_5\text{X}_5$ ($\text{X}=\text{Cl}$ or Br), we considered low-lying excitations and the magnetization process of a system of coupled tetrahedra built of four spins $S = 1/2$.

To investigate possible low-lying singlets and transitions between several ground states, we derived a classical Ising chain in a magnetic field as an effective Hamiltonian. Using it, we showed the growth of binding energy between singlet particles triggers a first-order transition between the simple rung-dimer (RD) phase and the spin-1 dimer (S1D) phase.

Most of excitations in the RD phase are immobile or strongly localized due to the geometry (the so-called ‘orthogonal dimer’ structure²⁸). On the other hand, in addition to immobile singlets, excitations with much larger mobility (with dispersion $\sim J_3$) are also allowed in the S1D phase. In both phases, there exists a ‘window’ in the vicinity of the point $J_1 = J_2$, where the lowest excitation is not a triplet, but many singlet excitations populate the gap to the lowest triplet. A similar situation is known to occur for a frustrated ladder ($J_2 = J_3 = J_4$)²⁹. In certain limits, these singlets can be viewed as bound states of dimer excitations. It would be worth mentioning here that these low-lying singlets in the S1D phase are *not* included in the Hilbert space of the effective spin-1 chain.

We also determined the phase boundary by two different methods (effective Hamiltonian and a numerical method) and compared the results to obtain satisfactory agreement. In particular, for a generalized coupling $J_3 \gg J_4$ we concluded that a weakly-coupled perfect ($J_1 = J_2$) tetrahedra is in the RD phase. As is suggested by this, the effect of couplings between tetrahedra (in particular, the resulting ground states) is sensitive to the detail of the couplings (*symmetric* or *generalized*, J_1 and J_2) and detailed information on the couplings is crucial in comparison with experiments.

One way to distinguish between two phases (RD and S1D) experimentally would be to use optical probes. For example, the Raman operator which creates singlet excitations belonging to A-representation of S_4 is given essentially by \mathcal{H}_1 with $J_3 = J_4$. Since it annihilates the RD ground state, the scattering intensity should be very weak for (cc)-polarization (c-axis is parallel to the chain axis), while it creates singlet combinations of two

‘ γ ’ tetrahedra in the S1D phase. (The Raman operator corresponding to B-representation takes the form $\sum_i K(\mathbf{S}_{1,i} - \mathbf{S}_{3,i}) \cdot (\mathbf{S}_{2,i+1} - \mathbf{S}_{4,i+1})$, which excites elementary singlets and two-triplet bound states both in the RD- and the S1D phase.)

In section III, we investigated the magnetization process. There appears a 1/2-plateau in the magnetization curve. In the dimer region $J_1 \gg J_2, J_3$, the plateau is accompanied by discrete symmetry (parity) breaking and is attributed to the ordered state: ...333333... or ...66666666..., whereas in the ‘ $S = 1$ ’ region a parity-symmetric state ...999999... realizes. Note that the translational symmetry is not broken at all. The transition between these two types of plateaus is described by a simple pseudo-spin ($S = 1$) Hamiltonian equivalent to the classical Blume-Capel model.

Finally, we give some brief comments on the effects of possible three-dimensional couplings which recent experiments⁶ suggest are relatively large. We carried out preliminary calculation assuming the simplest interchain coupling (J_\perp) compatible with the crystal structure and found the following: (i) the ground state problem is again described by the classical (3D) Ising model at least for small couplings and (ii) the phase boundary between RD- and S1D phase is relatively insensitive to the interchain coupling J_\perp . Therefore we may expect that if we are in the S1D phase when $J_\perp = 0$ then so are we even for small but finite $J_\perp (\neq 0)$. However, new phenomena show up when the dynamics in the triplet sector is considered. An analyses analogous to the one presented in section II B suggests that the triplet (‘9’) gap gets reduced substantially while the singlet-singlet gap slightly increases as we increase J_3 and J_\perp ; spin gaps in the *effective* spin-1 sector finally close and three-dimensional antiferromagnetic ordering may take place in the effective spin-1 system (not in the original spin-1/2 system). A similar phenomenon has been used as a theoretical trick in the context of the so-called composite-spin models^{30,31}. The region of the above ordered phase blows up from the transition line between S1D and Haldane (see Fig.4) and grows as J_\perp is increased.

Acknowledgments

This work was supported by the German Federal Ministry for Education and Research (BMBF) under the contract 03MI5HAN5. The hospitality and support of Hahn-Meitner-Institut Berlin, where this work was completed, is gratefully acknowledged. The authors thank W. Brenig, A. Harrison, F. Mila, Y. Nishiyama, and T. Vecua for discussions. They are also grateful to P. Lemmens and P. Millet for discussions and helpful correspondences.

* Present address:
Department of Physics, Aoyama Gakuin University tot-

- ¹ C. Lhuillier, P. Sindzingre, and J-B. Fouet. *cond-mat/0009336*;
R. Moessner. *cond-mat/0010301*.
- ² M.P. Gelfand. *Phys.Rev.B* **43**, 8644 (1991);
B. Sutherland. *Phys.Rev.B* **62**, 11499 (2001)
- ³ I. Bose and S. Gayen, *Phys.Rev.B* **48**, 10653 (1993);
A.K. Kolezhuk and H-J. Mikeska. *Int.J.Mod.Phys.B*, **12**, 2325 (1998).
- ⁴ M. Johnsson, K.W. Törnroos, F. Mila, and P. Millet. *Chem.Mater.*, **12**, 2853 (2000).
- ⁵ W. Brenig and K.W. Becker. *Phys.Rev.B*, **64**, 214413 (2001).
- ⁶ P. Lemmens et al. *Phys.Rev.Lett.*, **87**, 227201 (2001).
- ⁷ Y. Xian. *Phys.Rev.B*, **52**, 12485 (1995);
X. Wang. *cond-mat/9803290*.
- ⁸ F.D.M. Haldane. *Phys.Rev.Lett.*, **50**, 1153 (1983).
- ⁹ Y. Kato and Y. Tanaka. *J.Phys.Soc.Jpn.*, **63**, 1277 (1994);
S. Yamamoto. *Phys.Rev.B*, **52**, 10170 (1995).
- ¹⁰ K. Totsuka, Y. Nishiyama, N. Hatano, and M. Suzuki. *J.Phys.condensed matter*, **7**, 4895 (1995).
- ¹¹ M. den Nijs and K. Rommelse. *Phys.Rev.B* **40**, 4709 (1989);
S.M. Girvin and D. Arovas. *Phys.Scr.T*, **27**, 156 (1990).
- ¹² Actually, we carried out cluster expansion up to $(J_3/J_2)^5$ to find that a tiny discrepancy between analytic- and numerical results was removed by including the third-order correction.
- ¹³ M. Mambrini, J. Trébosch, and F. Mila. *Phys.Rev.B*, **59**, 13806 (1999).
- ¹⁴ P. Lecheminant et al. *Phys.Rev.B*, **56**, 2521 (1997);
C. Waldtmann et al. *Euro.Phys.J.B*, **2**, 501 (1998).
- ¹⁵ A.P. Ramirez, B. Hessen, and M. Winklemann. *Phys.Rev.Lett.*, **84**, 2957 (2000);
P. Sindzingre et al. *ibid.* **84**, 2953 (2000).
- ¹⁶ V.N. Kotov and O.P. Sushkov. *Phys.Rev.B*, **61**, 11820 (2000).
- ¹⁷ V.N. Kotov, J. Oitmaa, O. Sushkov, and Z. Weihong. *Phil.Mag.B*, **80**, 1483 (2000).
- ¹⁸ V.N. Kotov, M.E. Zhitomirsky, and O.P. Sushkov. *Phys.Rev.B*, **63**, 064412 (2001).
- ¹⁹ This localization must be closely related to the non-existence of the so-called $S = 1/2$ edge states in the $S = 1$ dimer phase⁹. If we weaken dimerization to enter the Haldane phase, the edge states show up and this type of excitations will dissociate into two $S = 1/2$ objects.
- ²⁰ D.C. Mattis. *The theory of magnetism*, Springer-Verlag, 1981.
- ²¹ For example, in the decoupling limit $J_3 = 0$ we can trace a level corresponding to a ‘ α ’ tetrahedron as we cross $J_2 = J_{2,c} = 1$. When $J_3 > 0$, however, an excited state corresponding to one ‘ α ’ tetrahedron in the RD background and that in the sea of ‘2’ tetrahedra should be considered quite different from each other.
- ²² A. Honecker, F. Mila, and M. Troyer. *Euro.Phys.J. B* **15**, 227 (2000).
- ²³ see for example, J.L. Cardy. *Scaling and renormalization in statistical physics*, Cambridge University Press, 1996.
- ²⁴ N. Okazaki, J. Miyoshi, and T. Sakai. *J.Phys.Soc.Jpn.* **69**, 3 (2000).
- ²⁵ K. Totsuka. *Phys.Rev.B* **57**, 3454 (1998).
- ²⁶ T. Tonegawa, M. Nakao, and M. Kaburagi. *J.Phys.Soc.Jpn.* **65**, 3317 (1996).
- ²⁷ K. Totsuka. *Phys.Lett.A* **228**, 103 (1997).
- ²⁸ S. Miyahara and K. Ueda. *Phys.Rev.Lett.* **82**, 3701 (1999);

- K. Totsuka, S. Miyahara, and K. Ueda. *ibid* **86**, 520 (2001).
- ²⁹ V.N. Kotov, O.P. Sushkov, and R. Eder. *Phys.Rev.B* **59**, 6266 (1999).
- ³⁰ J. Timonen and A. Luther. *J.Phys.C* **18**, 1439 (1985);
J. Solyom and J. Timonen. *Phys.Rev.B* **40**, 7150 (1089).
- ³¹ A. Koga and N. Kawakami. *Phys.Rev.B* **61**, 6133 (2000).

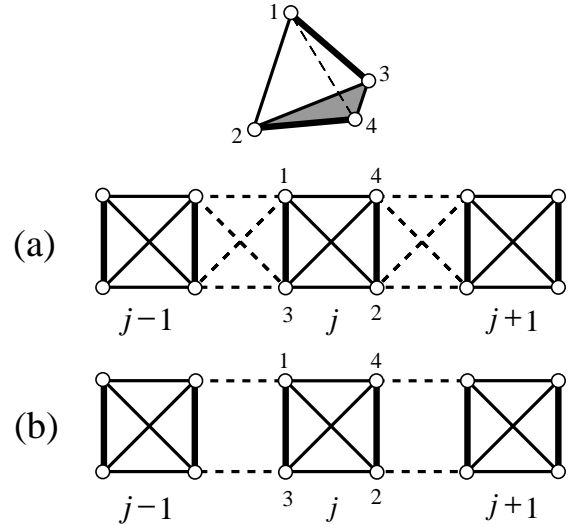


FIG. 1: Spin tetrahedron and two models considered in the text: symmetric model (a) and generalized model (b).

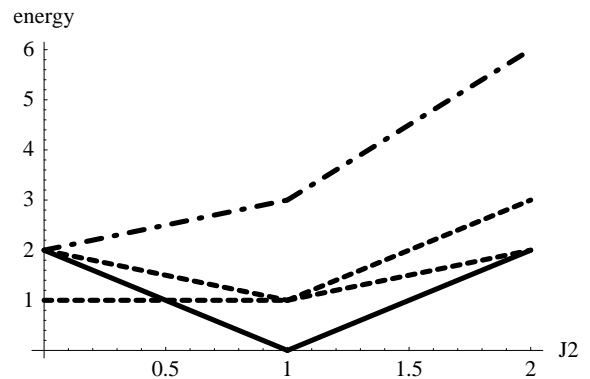


FIG. 2: Energy levels (in unit of J_1) of a single tetrahedron: singlet (solid), triplet (broken), and quintet (dot-dashed). Energy is measured from the ground state. Note that the ground state changes at $J_1 = J_2$.

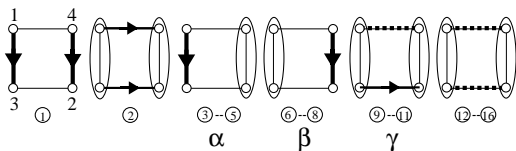


FIG. 3: Eigenstates of a single tetrahedron. Singlets: 1 (SD) and 2 (S1D), triplets: $\alpha = (3, 4, 5)$, $\beta = (6, 7, 8)$, and $\gamma = (9, 10, 11)$, quintet: $(12, 13, 14, 15, 16)$. Arrows denote singlets and dashed lines and ovals triplets. In the dimer picture, ‘2’, ‘9’-‘11’, and ‘12’-‘16’ can be viewed as 2-triplet bound states.

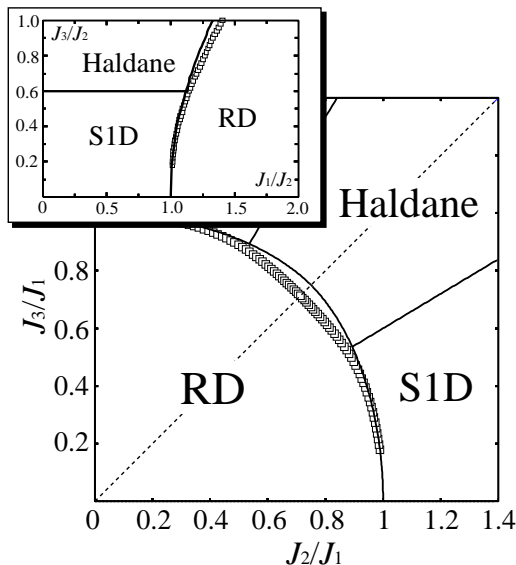


FIG. 4: Ground-state phase diagram for the symmetric model ($J_3 = J_4$). Note that the phase diagram is symmetric under $J_2 \leftrightarrow J_3$. The phase boundary between RD- and Haldane phases as obtained from the effective Hamiltonian $\mathcal{H}_{\text{Ising}}$ (eq.4) is shown by a full line and that from numerical data (for 16 sites, or $N = 8$; Ref. 10) by open squares. The inset shows the same data using the parametrization adopted in Ref. 5.

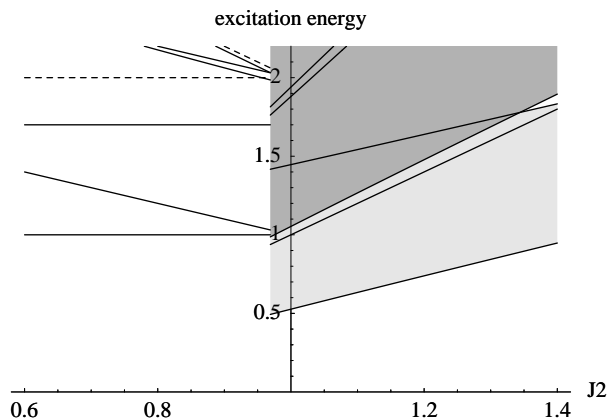


FIG. 6: Several low-lying triplets (in unit J_1) obtained by perturbation expansion in J_3 (some of them are exact) as a function of J_2/J_1 . Parameters are the same as in Fig.5. 1-triplet band and 2-triplet continuum are shown by light- and dark gray regions. Note that the dispersion of the lowest triplet suddenly changes at the transition since the ground states on both sides are completely different.

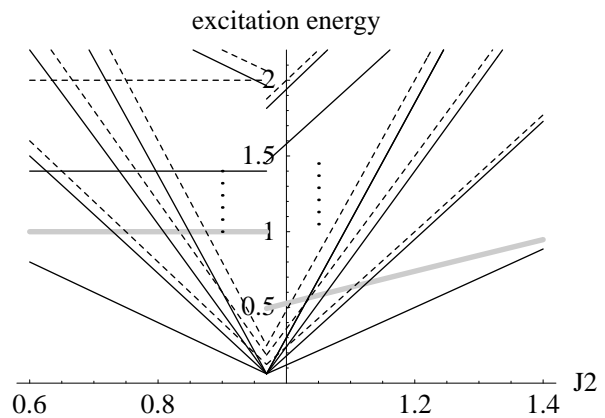


FIG. 5: Several low-lying singlets (in unit J_1) obtained by perturbation expansion in J_3 (some of them are exact) as a function of J_2 (J_3 is fixed). We chose $J_3 = 0.3J_1$ (hence first-order transition occurs at $J_2/J_1 = j_c = 0.96904\dots$). Elementary singlet and bound states are shown by solid line, while scattering states are shown by broken lines. Note that we show only a part of the entire singlet spectrum and actually a gap between the singlet ground state and the lowest triplet (shown by gray lines) is filled up with singlets composed of the elementary singlet discussed in section II.A.1.

phase	energy	spin	degeneracy	symmetry at Γ
RD	$\Delta_{\text{sing}}^{\text{RD}}$ (see eq.(7))	singlet	N	B
	$\Delta_{\text{sing}}^{\text{RD}} + 2(n-1) h_{\text{IM}} $	singlet	N	A (n :even) B (n :odd)
	$2N h_{\text{IM}} $	singlet	1	
	J_1	triplet	N	E
	$2J_1 - J_{2,3}$	triplet	N	A
S1D	$\Delta_{\text{S1D}}^{\text{sing}}$	singlet	N	B
	$\Delta_{\text{S1D}}^{\text{sing}} + 2(n-1)h_{\text{IM}}$	singlet	N	A (n :even) B (n :odd)
	$\Delta_{\text{type-1}}^{\text{triplet}}$	triplet	N	E
	$\Delta_{\text{type-2}}^{\text{triplet}}$	triplet	non-degen. band	B

TABLE I: Energy, spin, degeneracy, and symmetry classification (in terms of S_4) of typical excitations. N denotes the number of tetrahedra.

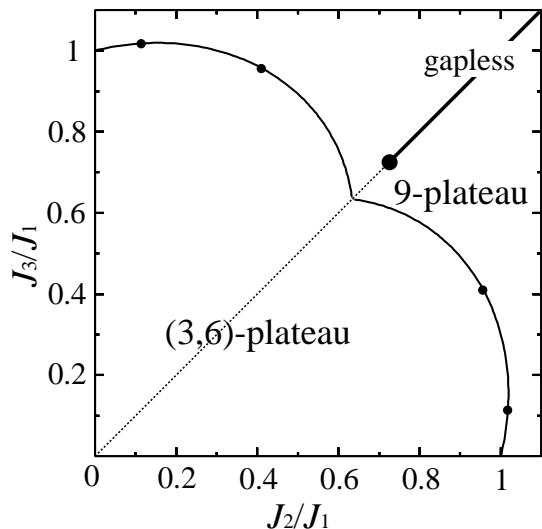


FIG. 7: Phase diagram for $m^z/m_{\text{sat}} = 1/2$ obtained by low-order perturbation. Inside the boundary, (3,6)-plateau occurs. Transition points determined by a similar method to that used in section I are plotted by small dots (numerical data were taken from Ref.26). A large dot on the symmetric line, which separates (3,6)-plateau- and non-plateau phases (shown by a thick line), was taken from Ref.22. From the results for the bond-alternating $S = 1$ chain^{26,27}, we believe that the non-plateau phase is realized *only* on the symmetric line. Poor convergence around the symmetry axis $J_2 = J_3$ may be attributed to the proximity to the criticality.